Temperature and time dependent magnetic phenomena in a nearly stoichiometric Ni_2MnGa alloy

2009 J. Phys.: Condens. Matter 21 026020

(http://iopscience.iop.org/0953-8984/21/2/026020)

J. Phys.: Condens. Matter **21** (2009) 026020 (7pp) doi:10.1088/0953-8984/21/2/026020

Temperature and time dependent magnetic phenomena in a nearly stoichiometric Ni_2MnGa alloy

C Gómez-Polo[1], J I Pérez-Landazabal[1], V Recarte[1], V Sánchez-Alarcos[1] and V A Chernenko[2]

[1] Departamento de Física, Universidad Pública de Navarra, Campus de Arrosadía 31006 Pamplona, Spain
[2] Institute of Magnetism, National Academy of Sciences of Ukraine, Vernadsky Street 36B, 03142 Kiev, Ukraine

Received 10 September 2008, in final form 4 November 2008
Published 11 December 2008
Online at stacks.iop.org/JPhysCM/21/026020

Abstract
In this work, the temperature and time dependence of the magnetic properties of a polycrystalline $Ni_{49.7}Mn_{24.1}Ga_{26.2}$ alloy is analysed. The law of approach to magnetic saturation has been employed to estimate the magnetic anisotropy in the three structural phases of the alloy (martensitic, pre-martensitic and austenitic). The temperature dependences of magnetic parameters, such as the magnetic susceptibility and coercive field, are interpreted in terms of the changes in the magnetic anisotropy taking place with the structural transformations. The strong magnetocrystalline anisotropy is confirmed to mainly control the magnetic response of the low temperature martensitic phase. Furthermore, magnetic relaxation studies (magnetic after-effect) have been employed to analyse the main differences between the magnetization processes in the three characteristic structural phases. The time decay of the magnetization displays a distinctive response in the pre-martensitic state. The results (logarithmic time decay of the remanent magnetization and field dependence of the magnetic viscosity) indicate the thermally activated nature of the relaxation process.

1. Introduction

Thermoelastic martensitic transformations in intermetallic alloys have been extensively studied during the last decades [1]. Among them, the stoichiometric Heusler Ni_2MnGa alloy stands out, where a displacive and diffusionless martensitic transformation (MT) from a high symmetry cubic structure (austenitic phase) to a low symmetry structure (martensitic phase) takes place upon cooling around $M_S \approx 220$ K [2]. In these martensitic Heusler alloys, large magnetic-field-induced strains of 6–10% [3–5] can be obtained by the re-orientation of the martensitic variants, enabling them to be employed in advanced magnetostrictive actuators and sensors. Alongside the extraordinary magnetostrictive characteristics, these ferromagnetic shape memory alloys (FSMAs) have been the subject of extensive basic research due to their complex non-trivial transformation behaviour (see, e.g., [6–9]). Upon cooling, the formation of a particular martensitic phase largely depends on the alloy composition (electron concentration per atom, e/a). Those alloys with e/a $<$ 7.7 display the MT below the Curie temperature, T_C, of the austenitic phase, while for alloys with e/a $>$ 7.7 the alloy undergoes the ferro–paramagnetic transition in the martensitic state [10]. As a rule, the former alloys ($M_S < T_C$) exhibit five-layered 10M- and/or seven-layered 14M-martensitic structures and those alloys with $M_S > T_C$ are characterized by a non-modulated 2M-martensite [11]. Besides, in the low temperature alloys including the stoichiometric Ni_2MnGa (e/a $<$ 7.7), the martensitic transition is preceded by a weakly first-order pre-martensitic phase transformation into an intermediate modulated pre-martensitic phase, *I* [9]. Its occurrence is mainly linked to the temperature softening of the TA_2 phonon branch [12], leading to a parallel softening in the elastic constants in the cubic phase.

Large magnetic field-induced strains (MFIS) in the martensitic phase are the result of the twin boundary motion under the driving force of the Zeeman energy, giving rise to an increase of the volume fraction of variants with the easy axis parallel to the applied magnetic field [13]. Thus, the magnetocrystalline anisotropy, *K*,

plays a remarkable role in the MFIS process. Strong magnetocrystalline anisotropy is required to make the movement of the twin boundaries energetically favourable in comparison with the magnetization rotation within the twins. The determination of K of the martensitic phase has been mainly performed (i) by the analysis of the magnetization curves along the hard and easy axes in single crystals [3, 4, 14–17], (ii) through the estimation of the anisotropy field from the magnetization curves in single crystalline [18–20] and polycrystalline samples [21–25], and (iii) by ferromagnetic resonance [26, 27]. However, in spite of the remarkable role of K, few reports analyse in detail its temperature dependence in both the martensitic and austenitic states. Although low values of the magnetocrystalline anisotropy in the austenitic phase are widely accepted, its actual estimation has been roughly analysed in the literature [14, 26, 27]. Furthermore, the occurrence of the intermediate modulated pre-martensitic phase in the low temperature alloys (e/a $<$ 7.7) causes a distinctive magnetic response. In particular, a clear dip in the magnetic susceptibility around the pre-martensitic transformation temperature, T_I, has been experimentally found [28–32]. Despite the essential contribution of the magnetoelastic coupling to the phonon instability [33, 34], the analysis of the basic magnetic characteristics of the intermediate modulated phase, such as the magnetic anisotropy, has been scarcely undertaken.

Accordingly, the main aim of the work is the analysis of the temperature and time dependence of the magnetization process in the three phases exhibited by a representative $Ni_{49.7}Mn_{24.1}Ga_{26.2}$ (e/a = 7.44) polycrystalline alloy. A different approach has been employed to estimate the temperature dependence of the magnetocrystalline anisotropy: the law of approach to magnetic saturation. The high field magnetization has been used to analyse the magnetic anisotropy contribution in both the martensitic and austenitic phases as well as in the intermediate pre-martensitic state. The results confirm the outstanding role of the magnetocrystalline anisotropy in the magnetic response of the low temperature martensite phase. Moreover, magnetic relaxation (magnetic after-effect) studies have been carried out to further analyse the main differences between the magnetization process in the three characteristic structural phases: austenite, pre-martensite and martensite. The magnetic viscosity coefficient, S, has been determined through the logarithmic time decay of the thermoremanent magnetization. A distinctive magnetic behaviour between the pre-martensitic and austenitic states is found in the magnetic relaxation response. From a technological point of view, the analysis of magnetic after-effects could be of great significance in the understanding of the dynamics of the magnetic-field-induced strains in the martensitic phase.

2. Experimental procedure

A nearly stoichiometric $Ni_{49.7}Mn_{24.1}Ga_{26.2}$ (at.%) polycrystalline alloy exhibiting the three characteristic phases was chosen as a model object for magnetic studies. The alloy composition was determined by x-ray fluorescence analysis. An ingot of 150 g was prepared by induction melting and casting into copper mould. As a result, the radial columnar morphology of crystallites with a few millimetres length and cross-section of a few tens of micrometres is usually formed [35]. Similar columnar structures are reported in Ni–Mn–Ga alloys obtained through arc-melting [36, 37]. The magnetic characterization was carried out with a Quantum Design MPMS XL-7 SQUID magnetometer and its AC magnetic susceptibility option [38]. Previous resonant ultrasound spectroscopy (RUS) and AC magnetic susceptibility results indicate that the martensitic transformation is characterized by the start and finish transformation temperatures M_s = 100 K, M_f = 75 K upon cooling, A_s = 107 K, A_f = 130 K upon heating, respectively, with a marked hysteresis of 35 K [39].

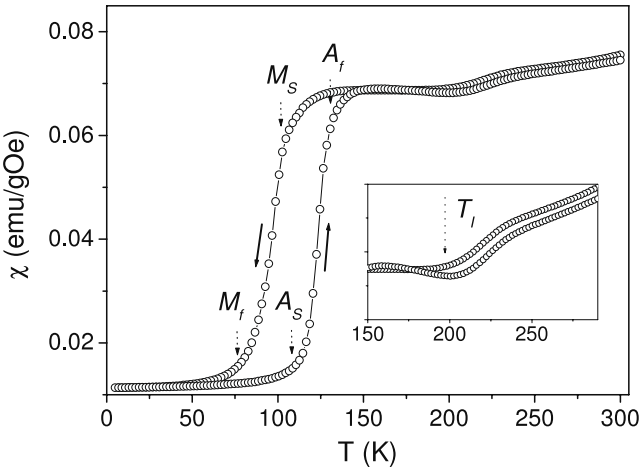

Figure 1. Temperature dependence of the AC magnetic susceptibility, χ, measured under a 3.5 Oe oscillating field (f = 1 Hz).

3. Experimental results and discussion

3.1. Temperature dependence of the hysteresis loops

Figure 1 shows the temperature dependence of the AC magnetic susceptibility, χ, obtained at an amplitude of the exciting AC magnetic field of 3.5 Oe and a frequency of 1 Hz. As previously reported (see, e.g., [18, 23, 29, 31]), upon cooling, the martensitic transformation is accompanied by a sharp decrease in χ that must be associated with the increase in the magnetocrystalline anisotropy in the martensitic phase. The wide martensitic transformation (around 25 K) would indicate the occurrence of some structural inhomogeneity in this polycrystalline sample. Furthermore, a small dip is clearly detected (see the inset of figure 1) around 200 K, correlated, according to the previous elastic characterization [39], with the first-order pre-martensitic transformation at T_I.

The temperature dependence of the coercive field, H_C (see figure 2(a)), obtained upon heating from the isothermal hysteresis loops at a maximum applied magnetic field of 6 T

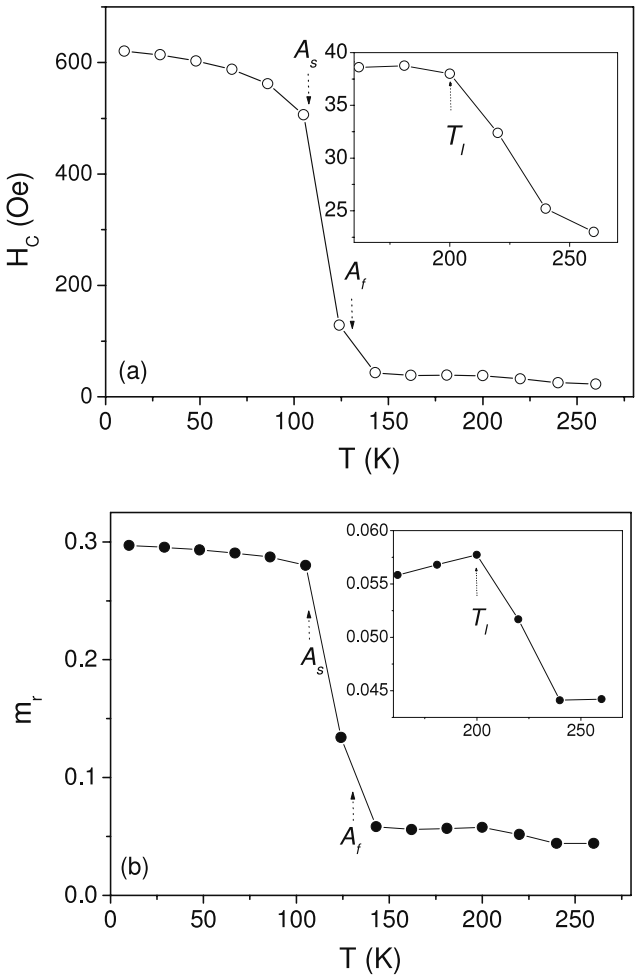

Figure 2. Temperature dependence upon heating of (a) the coercive field, H_C, and (b) the reduced remanence, $m_r = M_r/M_{6\,T}$ (M_r, magnetization at the remanence; $M_{6\,T}$, high field magnetization).

confirms the previous $\chi(T)$ characterization. A remarkable decrease for $T > A_S$ is experimentally detected, that must be associated with the reduction in the mean magnetocrystalline anisotropy as the reverse martensitic transformation proceeds. Besides this, the pre-martensitic precursor phase (I) can be clearly detected for $A_f < T < T_I$ as an anomalous constant value of H_C (see inset of figure 2(a)). For $T > T_I$ the sharper decrease of H_C with T reflects, as $\chi(T)$ does, a different magnetic behaviour in the high temperature parent (austenitic) phase.

Similarly, the temperature dependence of the magnetization at the remanence, M_r, normalized to the high field magnetization, $M_{6\,T}$ ($m_r = M_r/M_{6\,T}$) confirms the previous $\chi(T)$ and $H_C(T)$ results. As figure 2(b) shows, the appearance of the pre-martensitic precursor phase can be easily deduced from the m_r data. Firstly, the drastic decrease in m_r for $T > A_S$ should be ascribed to the enhancement of the demagnetization contribution as a consequence of the magnetic softening of the sample. Thus, the detectable increase in $m_r(T)$ for $A_f < T < T_I$ (see the inset of figure 2(b)) would confirm the slight magnetic hardening of the pre-martensitic precursor phase (I) with respect to the high temperature austenitic phase.

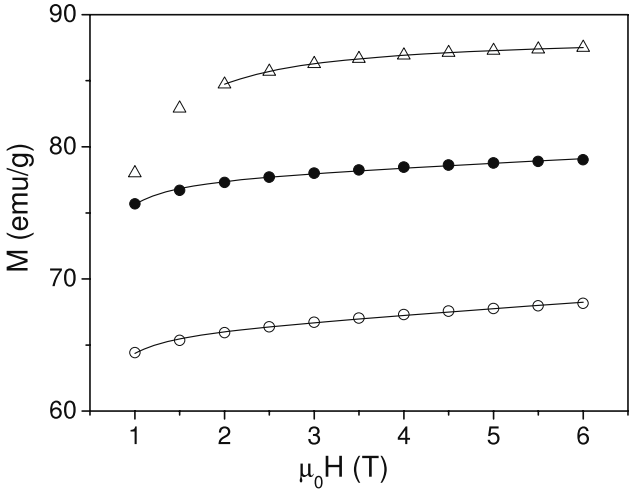

Figure 3. High field magnetization curves at $T = 10$ K (△), $T = 190$ K (●) and $T = 270$ K (○).

3.2. High field magnetization curves (approach to saturation)

In order to analyse in further detail the main differences in the magnetic behaviour of the three characteristic structural phases of the alloy (martensitic, pre-martensitic and austenitic), the high field magnetization curves (1 T $\leqslant \mu_0 H \leqslant$ 6 T) were determined at different measuring temperatures. Figure 3 shows the M–H curves at some selected temperatures: $T =$ 10 K (martensite), $T =$ 190 K (pre-martensite) and $T =$ 270 K (austenite). As expected, a higher magnetic field is required to reach the approach to saturation regime in the low temperature martensitic phase. These high field magnetization curves can be analysed in terms of the law of approach to saturation [40–44]:

$$M(H) = M_{ST}\left(1 - \frac{a}{H} - \frac{b}{H^2}\right) + \chi_{hf} H \qquad (1)$$

where M_{ST} is the saturation magnetization and χ_{hf} the high field susceptibility resulting from the increase in the spontaneous magnetization by the application of the magnetic field. The term a/H is usually associated with the contribution of local inhomogeneities (i.e. structural defects, non-magnetic inclusions or microstresses), while b/H^2 is correlated with the effect of the magnetocrystalline anisotropy. In the present case, as the solid line of figure 3 shows, the high field magnetization curves can be suitably fitted to the approach to saturation law (equation (1)). Due to the higher magnetic field required to saturate the sample in the low temperature martensitic state, the fitting is restricted to $\mu_0 H \geqslant 2$ T in this low temperature range ($T \leqslant A_S$).

In the whole measuring temperature range (10 K $\leqslant T \leqslant$ 290 K), a high field susceptibility contribution should be considered, monotonically increasing with T and ranging from 4.8×10^{-6} emu g^{-1} Oe^{-1} for the low temperature martensitic state ($T =$ 10 K) to 5×10^{-5} emu g^{-1} Oe^{-1} at $T =$ 290 K (austenitic phase). The obtained χ_{hf} values are in accordance with those reported in some other highly anisotropic ferromagnets (i.e. NdFeB hard magnets [41]).

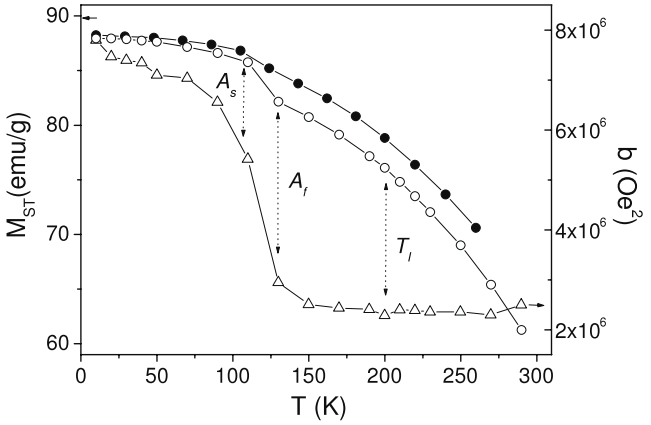

Figure 4. Saturation magnetization, M_{ST} (magnetization under an applied magnetic field $\mu_0 H = 6$ T), versus temperature, T (●). Temperature dependence of approach to saturation fitting parameters: M_{ST} (○) and b (△) (see equation (1)).

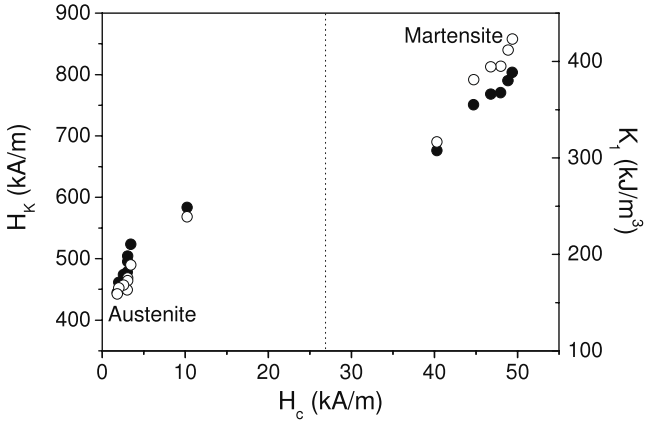

Figure 5. The anisotropy field, H_k (○), and the magnetocrystalline anisotropy constant, K_1 (●), versus the coercive field, H_C.

With respect to the a/H term, its contribution is much smaller (almost negligible) at high measuring temperatures, that is, for the pre-martensitic and austenitic phases, than at low temperatures. In the low temperature region the best fitting is obtained considering a nearly constant (temperature independent) a value close to 380 Oe for the martensitic phase. This result clearly points out the difference in the microstructure characteristics of the low temperature martensitic phase. In this case, the twinned structure would enhance the contribution of local inhomogeneities (microstress distribution).

Figure 4 shows the temperature dependence of the fitting M_{ST} and b parameters (equation (1)) obtained from the isothermal high field magnetization curves (upon heating). For comparison, the magnetization at $\mu_0 H = 6$ T obtained from the previous hysteresis loop characterization (section 3.1) is also plotted as closed circles. As figure 4 shows, the martensitic transformation can be clearly detected as a noticeable decrease in M_{ST} for $A_s \leqslant T \leqslant A_f$. However, $M_{ST}(T)$ does not display any anomaly in the vicinity of the pre-martensitic transition ($T \approx T_I$). With respect to the magnetic anisotropy contribution, $b(T)$, a similar conclusion can be outlined: a sharp decrease for $T \geqslant A_S$ and negligible changes in its temperature dependence around the pre-martensitic phase transformation. These results indicate that the occurrence of the pre-martensitic precursor would mainly determine the low field magnetic response of the alloy, but scarcely modify the high field magnetic parameters in this pre-martensitic transition temperature range. As suggested in [28], the appearance of the micromodulated elastic domains would give rise through the magnetoelastic interaction to the detected changes in the magnetization process of the intermediate phase (i.e. dip in the magnetic susceptibility around T_I). The antiphase domains formed during the pre-martensitic transition would act as additional structural defects (i.e. pinning centres) for the domain wall displacements. Moreover, an increase in the saturation magnetostriction in a nearly stoichiometric Ni_2MnGa alloy around T_I has been reported [34]. This increase in the magnetoelastic anisotropy term would contribute to the hindrance of the domain wall movement and thus to the observed magnetic hardening associated with the appearance of the pre-martensitic precursor (see figures 1 and 2).

As previously indicated, the b coefficient can be directly related to the magnetocrystalline anisotropy. In the case of a polycrystalline uniaxial ferromagnetic material, the following relationship holds [42]:

$$b = \frac{4K_1^2}{15M_{ST}^2} \tag{2}$$

where K_1 is the first-order uniaxial anisotropy constant and higher-order terms are neglected (K_2). Figure 5 shows the anisotropy constant, K_1 (solid symbols), and the associated anisotropy field, $H_K = \frac{2K_1}{\mu_0 M_{ST}}$ (open symbols), as a function of the coercive field, H_C. As expected from figure 4, the highest magnetocrystalline anisotropy constant ($K_1 = 380$ kJ m^{-3} at 10 K) is achieved in the low temperature martensitic phase. In fact, similar values ($K_1 \approx 400$ kJ m^{-3}) are reported in Ni_2MnGa and nearly stoichiometric alloys [15, 20]. On the other side, the high temperature austenitic phase displays anomalous high K_1 values ($K_1 \approx 160$ kJ m^{-3} at 260 K), just approximately half those found in the high anisotropy martensitic phase. Moreover, the assumed uniaxial nature of the ferromagnetic phases in the performed magnetic characterization should be noted (see equation (2)). Although this assumption is valid in the tetragonal 10M martensitic phase, it should be revised for the cubic pre-martensitic and austenitic phases. For these cases, the assumption of a cubic magnetic structure would give rise to even higher K_1 values, since in cubic ferromagnetic materials the following relationship holds: $b = \frac{8K_1^2}{105M_{ST}^2}$ [40].

The occurrence of a certain preferential grain growth (i.e. columnar growth) along a certain direction of the cubic structure [35–37] would explain the above described effects, that is, the large effective magnetic anisotropy constant and the uniaxial magnetic nature of the pre-martensitic and austenitic phases. The magnetostatic energy of elongated crystalline grains would contribute to the effective magnetic anisotropy

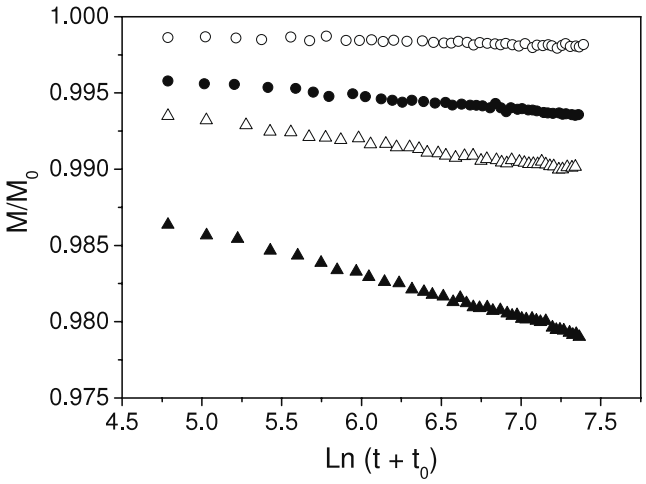

Figure 6. Magnetization decay (M versus $Ln(t + t_0)$, $t_0 = 120$ s) obtained under a cooling field $H_{cool} = 1000$ Oe at different measuring temperatures, T: 20 K (○), 70 K (●), 120 K (△) and 260 K (▲). The magnetization data are scaled to the initial magnetization, M_0.

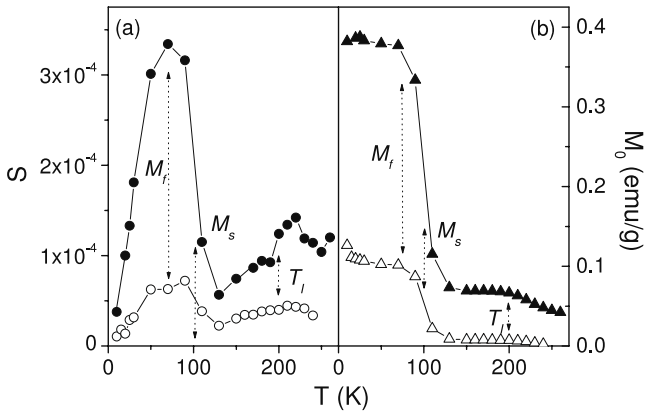

Figure 7. Temperature dependence of the (a) viscosity coefficient, S, and (b) initial remanent magnetization, M_0, obtained at different cooling fields: open symbols, $H_{cool} = 100$ Oe; solid symbols, $H_{cool} = 1000$ Oe.

of the lower magnetocrystalline phases (pre-martensitic and austenitic), introducing a uniaxial magnetic character in the sample. However, in the high magnetocrystalline martensitic state this contribution can be considered nearly negligible and the magnetocrystalline anisotropy would mainly control the magnetic response of the sample. In this case, the characteristic twinned microstructure would also contribute to the averaging of the uniaxial character of the shape anisotropy term associated with the preferential crystalline growth.

On the other side, the magnetization process within the low field range mainly depends on the domain wall distribution that basically is the result of the counterbalance between the magnetocrystalline anisotropy and magnetostatic energy terms. However, as a general rule, H_C can be expressed as proportional to the anisotropy field, $H_C = \alpha H_K$, with α ranging from 0 to 0.5 ($\alpha = 0.5$ for magnetization coherent rotation). In the present case, the linear fit of H_C versus H_K leads to the following results:

$$\text{Martensitic } (T \leqslant A_s): H_C = 0.07 H_K \tag{3a}$$

$$\text{Pre-martensitic and austenitic } (T > A_s): H_C = 0.03 H_K + C; \quad C < 0. \tag{3b}$$

In both cases, the low α value ($\alpha \ll 0.5$) would confirm the dominant role of domain wall displacements in the magnetization process of the sample. In fact, image studies show that at low magnetic fields each variant in the martensitic state contains many small magnetic domains [45, 46], while large magnetic domains (~1–10 μm) are usually detected in the high temperature austenitic phase [47]. In the present case, the most remarkable result is the negative value of the C coordinate in the pre-martensitic and austenitic states (equation (3*b*)). Such a negative value would confirm the overestimation of H_K through the approach to saturation analysis. As previously discussed, a shape anisotropy contribution would explain the anomalous high values of the magnetic anisotropy in the high field region (single domain saturated state) for the cubic pre-martensitic and austenitic phases. However, its effect should be disregarded at low applied magnetic fields, where a multidomain structure appears and the domain wall displacements dominate the magnetization process of the sample.

3.3. Magnetic relaxation studies

Magnetic relaxation effects, that is, the time evolution of the isothermal magnetization, have been widely employed in different magnetic systems to analyse the dynamics of the irreversible magnetization [48–51]. Upon a change of magnetic field, the magnetization of a ferromagnetic system relaxes towards a new equilibrium state. In the case of domain wall movement, the magnetic relaxation in a ferromagnet usually arises due to thermally activated domain wall re-orientation processes.

In this work, the magnetic relaxation studies were carried out through the measurements of the remanent magnetization (magnetization M at $H = 0$) as a function of time, t, after having cooled the sample under constant magnetic field, H_{cool}, from 300 K to the measuring temperature. Figure 6 shows the magnetization decay (M as a function of $Ln(t + t_0)$, $t_0 = 120$ s) obtained under $H_{cool} = 1000$ Oe at different measuring temperatures, T. A linear behaviour of M versus $Ln(t + t_0)$ is found and thus the determination of the magnetic viscosity, S, can be performed according to the following relationship:

$$M(t) = M_0 - S Ln(t + t_0). \tag{4}$$

The logarithmic time dependence of the remanence is usually ascribed to thermally activated processes across a distribution of energy barriers. Figure 7 displays the temperature dependence of the (a) S and (b) M_0 parameters obtained at $H_{cool} = 100$ Oe (open symbols) and 1000 Oe (solid symbols) according to equation (4). The martensitic state ($T < M_s$) displays maximum values in the magnetic viscosity. Moreover, in a similar way to the data shown in figure 2(b) (m_r versus T), the martensitic transformation can

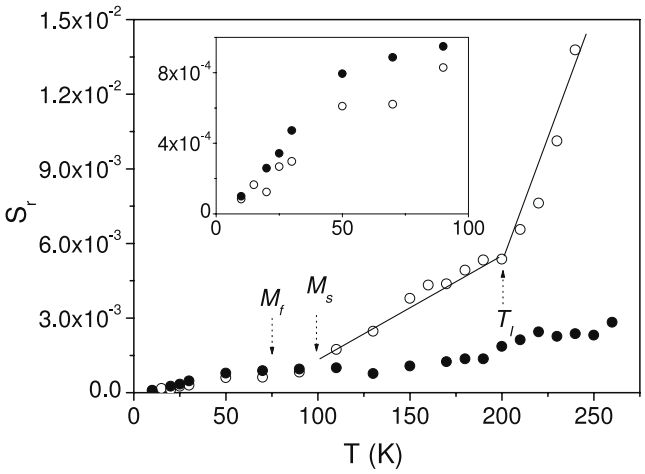

Figure 8. Normalized viscosity coefficient, $S_r = S/M_0$, as a function of temperature, T, for cooling fields $H_{cool} = 100$ Oe (○) and $H_{cool} = 1000$ Oe (●).

be clearly detected through a sharp decrease in the initial remanent magnetization, M_0, for $T \geqslant M_s$. However, with respect to the precursor pre-martensitic state, negligible changes can be detected in both S and M_0 parameters around T_I.

In order to discriminate those changes in the magnetic viscosity associated with the temperature dependence of the remanent magnetization, the normalized viscosity $S_r = S/M_0$ is defined and its temperature dependence calculated (see figure 8). A continuous increase in S_r with T is detected in the whole measuring temperature range, confirming the thermally activated nature of the relaxation phenomena (i.e. depinning of domain walls and nucleation of domains with reverse magnetization). In this thermally activated regime, maximum values in the relaxation contribution should be obtained for cooling fields around the sample coercivity, H_C. As previously analysed (see figure 2(a)), a remarkable increase in H_C is associated with the high magnetocrystalline anisotropy martensitic state (H_C(martensite) $\approx$ 600 Oe; H_C(pre − martensitic and austenite)$\approx$30 Oe). Therefore, an opposite trend in the temperature dependence of S_r should be obtained as function of the cooling field in the three structural states of the sample. As the inset of figure 8 shows, in the low temperature range ($T < M_f$, martensite phase) higher values of S_r are achieved for $H_{cool} = 1000$ Oe. In contrast, an enhancement in the relaxation phenomena (increase in S_r) is detected for the lower cooling field ($H_{cool} = 100$ Oe) in the austenitic and pre-martensitic phases.

Finally, the magnetic relaxation analysis confirms the different magnetic behaviour of the pre-martensitic precursor with respect to the high temperature austenitic phase. As figure 8 shows, the pre-martensitic transformation (T_I) can be clearly detected as a change in the slope of $S_r(T)$. This result would support the distinctive role of the pinning domain mechanisms (appearance of micromodulated elastic domains) in the magnetization process of the pre-martensitic precursor phase [28].

4. Conclusions

Three structural states and the phase transitions between them in a nearly stoichiometric Ni_2MnGa alloy have been characterized through the temperature and time dependent magnetic phenomena. The temperature dependences of the magnetization curves of a polycrystalline $Ni_{49.7}Mn_{24.1}Ga_{26.2}$ alloy were measured in the low and high field regimes. The estimation of the magnetocrystalline anisotropy is carried out through the analysis of the law of approach to magnetic saturation in the three structural phases of the alloy (martensitic, pre-martensitic and austenitic). The strong magnetocrystalline anisotropy mainly controls the magnetic response (i.e. magnetic susceptibility and coercive field) of the low temperature martensitic phase. The time decay of the thermoremanent magnetization is also analysed and compared with the previous magnetic characterization. The results (logarithmic time decay of the remanent magnetization and field dependence of the magnetic viscosity) indicate the thermally activated nature of the analysed relaxation processes. Relaxation parameters were shown to be additional tools to discern between the three studied phases.

Acknowledgments

This work has been carried out with the financial support of the Spanish Ministerio de Educación y Ciencia (project MAT2006-12838). VAC is grateful to the Fondazione Cariplo for financial support (project 2004.1819-A10.9251).

References

[1] Otsuka K and Kakeshita T (ed) 2002 Science and technology of shape memory alloys: new developments *MRS Bull.* **27** 81–160
[2] Webster P J, Ziebeck K R A, Town S L and Peak M S 1984 *Phil. Mag.* B **49** 295
[3] Murray S J, Marioni M, Allen S M and O'Handley R C 2000 *Appl. Phys. Lett.* **77** 886
[4] Sozinov A, Likhachev A A, Lanska N and Ullakko K 2002 *Appl. Phys. Lett.* **80** 1746
[5] Mullner P, Chernenko V A and Kostorz G 2004 *J. Appl. Phys.* **95** 1531
[6] Chernenko V A, Segui C, Cesari E, Pons J and Kokorin V V 1998 *Phys. Rev.* B **57** 2659
[7] Kuo Y K, Sivakumar K M, Chen H C, Su J H and Lue C S 2005 *Phys. Rev.* B **72** 054116
[8] Khovaylo V V, Buchelnikov V D, Kainuma R, Koledov V V, Ohtsuka M, Shavrov V G, Takagi T, Taskaev S V and Vasiliev A N 2005 *Phys. Rev.* B **72** 224408
[9] Chernenko V A, Pons J, Seguí C and Cesari E 2002 *Acta Mater.* **50** 53
[10] Chernenko V A 1999 *Scr. Mater.* **40** 523
[11] Pons J, Chernenko V A, Santamarta R and Cesari E 2000 *Acta Mater.* **48** 3027
[12] Zheludev A, Shapiro S M, Wochner P and Tanner L E 1996 *Phys. Rev.* B **54** 15045
[13] O'Handley R C 1998 *J. Appl. Phys.* **83** 3263
[14] Tickle R and James R D 1999 *J. Magn. Magn. Mater.* **195** 627
[15] Okamoto N, Fukuda T, Kakeshita T and Takeuchi T 2006 *Mater. Sci. Eng.* A **438–440** 948
[16] Jiang C, Wang J and Xu H 2005 *Appl. Phys. Lett.* **86** 252508
[17] Lian T, Jiang C and Xu H 2005 *Mater. Sci. Eng.* A **402** 5

[18] Heczko O, Straka L, Lanska N, Ullakko K and Enkovaara J 2002 *J. Appl. Phys.* **91** 8228
[19] Straka L, Heczko O and Ullakko K 2004 *J. Magn. Magn. Mater.* **272–276** 2049
[20] Straka L and Heczko O 2003 *J. Appl. Phys.* **10** 8636
[21] Wirth S, Leithe-Jasper A, Vasil'ev A N and Coey J M D 1997 *J. Magn. Magn. Mater.* **167** L7
[22] Albertini F, Morellon L, Algarabel P A, Ibarra M R, Pareti L, Arnold Z and Calestani G 2001 *J. Appl. Phys.* **89** 5614
[23] Albertini F, Besseghini S, Paoluzi A, Pareti L, Pasquale M, Passaretti F, Sasso C P, Stantero A and Villa E 2002 *J. Magn. Magn. Mater.* **242–245** 12421
[24] Albertini F, Pareti L, Paoluzi A, Morellon L, Algarabel P A, Ibarra M R and Righi L 2002 *Appl. Phys. Lett.* **81** 4032
[25] Albertini F, Paoluzi A, Pareti L, Solzi M, Righi L, Villa E, Besseghini S and Passaretti F 2006 *J. Appl. Phys.* **100** 023908
[26] Shanina B D, Konchits A A, Kolesnik S P, Gavriljuk V G, Glavatskij I N, Glavatska N I, Soderberg O, Lindroos V K and Foct J 2001 *J. Magn. Magn. Mater.* **237** 309
[27] Gavriljuk V G, Dobrinsky A, Shanina B D and Kolesnik S P 2006 *J. Phys.: Condens. Matter* **18** 7613
[28] Mañosa L, González-Comas A, Obradó E, Planes A, Chernenko V A, Kokorin V V and Cesari E 1997 *Phys. Rev.* B **55** 11068
[29] Khovailo V V, Takagi T, Bozhko A D, Matsumoto M, Tani J and Shavrov V G 2001 *J. Phys.: Condens. Matter* **13** 9655
[30] Zuo F, Su X and Wu K H 1998 *Phy. Rev.* B **58** 11127
[31] Wang W H, Chen J L, Gao S X, Wu G H, Wang Z, Zheng Y F, Zhao L C and Zhan W S 2001 *J. Phys.: Condens. Matter* **13** 2607
[32] Pérez-Landazábal J I, Sánchez-Alarcos V, Gómez-Polo C, Recarte V and Chernenko V A 2007 *Phys. Rev.* B **76** 092101
[33] Planes A, Obradó E, González-Comas A and Mañosa L 1997 *Phys. Rev. Lett.* **79** 3926
[34] Cui Y, Yang X, Kong C, Ma Y and Pan F 2006 *Solid State Commun.* **138** 234
[35] Vitenko I N, Zasimchuk I K, Kokorin V V and Chernenko V A 1989 *Metallofizika* **11** 65
[36] Gao Z Y, Zhao K, Chen F, Cai W, Zhao L C, Wu G H, Chen J L and Zhan W S 2003 *Mater. Sci. Technol.* **19** 691
[37] Rudajevova A, Frost M and Jäger A 2007 *Mater. Sci. Technol.* **23** 542
[38] UNPN-E007 Feder Project 2003
[39] Sánchez-Alarcos V, Pérez-Landazábal J I, Recarte V, Gómez-Polo C and Chernenko V A 2006 *Int. J. Appl. Electron. Mech.* **23** 93
[40] Chikazumi S 1964 *Physics of Magnetism* (New York: Wiley) p 274
[41] Andreev S V, Bartashevich M I, Pushkarsky V I, Maltsev V N, Pamyatnykh L A, Tarasov E N, Kudrevatykh N V and Goto T 1997 *J. Alloys Compounds* **260** 196
[42] Hernando A, Gómez-Polo C, El Ghannami M and García-Escorial A 1999 *J. Magn. Magn. Mater.* **173** 275
[43] Melikhov Y, Snyder J E, Jiles D C, Ring A P, Paulsen J A, Lo C C H and Dennis K W 2006 *J. Appl. Phys.* **99** 08R102
[44] Cullity B D 1972 *Introduction to Magnetic Materials* (Reading, MA: Addison-Wesley) p 347
[45] Chopra H D, Ji C and Kokorin V V 2000 *Phys. Rev.* B **61** R14913
[46] Ge Y, Heczko O, Söderberg O and Hannula S P 2006 *Scr. Mater.* **54** 2155
[47] Park H S, Murakani Y, Shindo D, Chernenko Va and Kanomata T 2003 *Appl. Phys. Lett.* **83** 3752
[48] Ibrahim M M, Darwish S and Seehra M S 1995 *Phys. Rev.* B **51** 2955
[49] Makhlouf S A 2004 *J. Magn. Magn Mater.* **272–276** 1539
[50] Jahn L, Schumann R and Rodewald W 1996 *J. Magn. Magn. Mater.* **153** 302
[51] Gao J H, Sun D L, Zhan Q F, He W and Cheng Z H 2007 *Phys. Rev.* B **75** 064421